Mem. S.A.It. Suppl. Vol. 21, 76

Memorie della
Supplementi

Population III Gamma-Ray Bursts

K. Toma[1], T. Sakamoto[2], and P. Mészáros[3]

[1] Department of Earth and Space Science, Osaka University, Toyonaka 560-0043, Japan
e-mail: `toma@vega.ess.sci.osaka-u.ac.jp`
[2] Center for Research and Exploration in Space Science and Technology (CRESST), NASA Goddard Space Flight Center, Greenbelt, MD 20771
[3] Department of Astronomy and Astrophysics, Pennsylvania State University, 525 Davey Lab, University Park, PA 16802, USA

Abstract. Population III stars are theoretically expected to be prominent around redshifts $z \sim 20$, consisting of mainly very massive stars (VMSs) with $M_* \gtrsim 100\ M_\odot$, but there is no direct observational evidence for these objects. They may produce collapsar gamma-ray bursts (GRBs), with jets driven by magnetohydrodynamic processes, whose total isotropic-equivalent energy could be as high as $E_{\rm iso} \gtrsim 10^{57}$ erg over a cosmological-rest-frame duration of $t_d \gtrsim 10^4$ s, depending on the progenitor mass. The detection of a burst with such a high total energy and a long duration would be a strong evidence for a VMS progenitor. We calculate the prompt emission and afterglow spectra of such Pop. III GRBs based on the standard models, and show that they will be detectable with the *Swift* BAT/XRT and *Fermi* LAT instruments. We also show that the late-time radio afterglows of Pop. III GRBs for typical parameters, despite the large distances, can be very bright: $\simeq 140$ mJy at 1 GHz, which may lead to a constraint on the Pop. III GRB rate from the current radio survey data, and $\simeq 2.4$ mJy at 70 MHz, which implies that Pop. III GRB radio afterglows could be interesting background source candidates for 21 cm absorption line detections.

Key words. black hole physics — dark ages, reionization, first stars — gamma rays burst: general — stars: Population III — X-rays: bursts — radio continuum: general — surveys

1. Introduction

Recent studies on cosmology and primordial star formation predict that the first generation of stars (population III stars) may be most prominent around $z \sim 20$, consisting of metal-poor, mainly very massive stars (VMSs) with $M_* \gtrsim 100\ M_\odot$ (e.g., Ciardi & Ferrara 2005). The details of how these processes unfold remain elusive, since observational data for redshifts $z \gtrsim 6$ are very limited. Observations of gamma-ray bursts (GRBs), however, may provide unique probes of the physical conditions of the universe at such redshifts. The GRB prompt emission and the afterglows were expected to be observable at least out to $z \gtrsim 10$. Currently the most distant burst that has been spectroscopically confirmed is GRB 090423 at $z \simeq 8.2$ (Tanvir et al. 2009; Salvaterra et al. 2009), indicating that GRB observations are very promising for exploring the high-redshift universe (see also Kawai et al. 2006; Greiner et al. 2009; Cucchiara et al. 2011).

One of the main questions that will be asked, if and when the redshift of a burst is determined to be $z \gtrsim 10$ (e.g. by observation of the Lyα cutoff at IR frequencies), is whether this burst is produced by a Pop. III VMS or not. An effective way to pinpoint a Pop. III progenitor is to examine whether the afterglow spectrum from its surrounding medium is devoid of metals through high-resolution IR and X-ray spectroscopy by ground-based facilities and/or future space experiments. Here we discuss in detail another way by estimating the duration and total energy of the jet through the X-ray and γ-ray observations of the afterglow and/or prompt emission. Very recently it has been actively discussed that the GRBs arising from Pop. III VMSs may have very different properties than the GRBs from Pop. I/II GRBs, i.e., having very large total energies and very long durations (e.g., Komissarov & Barkov 2010; Mészáros & Rees 2010; Fryer et al. 2001) (hereafter KB10, MR10, FWH01, respectively). We propose that the detection of a burst with a very high total isotropic-equivalent energy $E_{\rm iso} \gtrsim 10^{57}$ erg and a very long (cosmological rest frame) duration $t_d \gtrsim 10^4$ s would be strong evidence for a VMS progenitor.

In Section 2 we present the basic parameters of the Pop. III GRB jets. We calculate the prompt emission (in Section 3) and very early afterglow spectra (in Section 4) to show that the multiwavelength observations can constrain the energy scales and durations of Pop. III GRBs. We also show that the late-time radio afterglows may provide us important information in Section 5.

2. Pop. III GRB Jet Model

We consider VMSs rotating very fast, close to the break-up speed, as a representative case of Pop. III GRB progenitor stars. Those in the 140 $M_\odot \lesssim M_* \lesssim 260$ $M_\odot$ range are expected to explode as pair instability supernovae without leaving any compact remnant behind, while those in the $M_* \gtrsim 260$ $M_\odot$ range are expected to undergo a core collapse leading directly to a central BH, whose mass would itself be hundreds of solar masses (FWR01). Accretion onto such BHs could lead to collapsar GRBs (Woosley 1993). Prior to the collapse, the fast rotating VMSs may be chemically homogeneous and compact, without entering the red giant phase, so that the stellar radius is $R_* \simeq 10^{12}$ cm for $M_* \simeq 10^3$ $M_\odot$ (KB10).

For such large BH masses $M_h \gtrsim 100 M_\odot$, the density and temperature of the accretion disk are too low for neutrino cooling to be important, and the low neutrino release from the accretion disk is insufficient to power a strong jet (FWR01). The rate of energy deposition through this mechanism may be estimated by using the formula recently deduced by Zalamea & Beloborodov (2011) as $L_{\nu\bar{\nu}} \simeq 5 \times 10^{46}$ $\dot{M}_{-1}^{9/4} M_{h,2.5}^{-3/2}$ erg s^{-1}, where $\dot{M} = 0.1 \dot{M}_{-1} M_\odot$ s^{-1} is the accretion rate and $M_{h,2.5} = M_h/(10^{2.5} M_\odot)$. This is clearly insufficient for detection from such high redshifts. However, strong magnetic field build-up in the accretion torus or disk could lead to much stronger jets, dominated by Poynting flux. Such jets will be highly relativistic, driven by the magnetic extraction of the rotational energy of the central BH through the Blandford-Znajek (BZ) mechanism (Blandford & Znajek 1977). The luminosity extracted from a Kerr BH with dimensionless spin parameter a_h threaded by a magnetic field of strength B_h is $L_{\rm BZ} \approx (a_h^2/128) B_h^2 R_h^2 c$, where $R_h \approx GM_h/c^2$ is the event horizon radius of the BH. The dynamics of the radiatively inefficient accretion disk may be described (KB10) through advection-dominated (ADAF) model (Narayan & Yi 1994). For a VMS rotating at, say, half the break-up speed, the disk outer radius will be $R_d \simeq R_*/4$, and for a disk viscosity parameter $\alpha = 10^{-1}\alpha_{-1}$, the accretion time $t_d \simeq (7/3\alpha)(R_d^3/GM_h)^{1/2}$ is calculated as

$$t_d \simeq 1.4 \times 10^4 \ \alpha_{-1}^{-1} R_{*,12}^{3/2} M_{h,2.5}^{-1/2} \ {\rm s}, \tag{1}$$

where we have defined $R_{*,12} = R_*/10^{12}$ cm. This gives an estimate for both the disk lifetime and the duration of the jet, in the source frame. The intrinsic jet duration $t_d \simeq 10^4$ s is sufficient to break through the star (Suwa & Ioka 2010; Nagakura et al. 2011). The poloidal magnetic field strength in the disk should scale with the disk gas pressure, P, so that $B_h^2 = 8\pi P/\beta$, where $\beta = 10$ β_1 is the magnetization parameter. Combining these equations result in a jet luminosity as $L_{\rm BZ} \simeq (14/96)(a_h^2/\alpha\beta)\dot{M}c^2 \simeq$

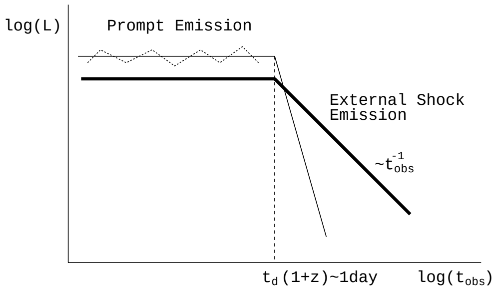

Fig. 1. Schematic figure of the bolometric luminosity evolutions of the external shock emission (thick line) and the prompt emission (thin line) as functions of time from the onset of the prompt emission. The prompt emission may involve some variability, which is shown by the dotted line.

2.2×10^{51} $(a_h^2/\alpha_{-1}\beta_1)M_{d,2.5}t_{d,4}^{-1}$ erg s^{-1}, where we have assumed a constant accretion rate $\dot{M} \simeq M_d/t_d$, and $M_d = 10^{2.5}M_{d,2.5}M_\odot$ is the total disk mass.

The total extracted energy during the accretion time t_d is then $E_{\rm BZ} \simeq (\sqrt{14}/96)(a_h^2/\alpha\beta)M_d c^2$. Assuming that the jet has an opening angle of $\theta_j = 0.1\ \theta_{j,-1}$, we can then write the total isotropic-equivalent energy of the jet as (Toma et al. 2011a)

$$E_{\rm iso} \simeq 4.4 \times 10^{57}\ \frac{(1-\epsilon_\gamma)a_h^2}{\alpha_{-1}\beta_1} M_{d,2.5}\theta_{j,-1}^{-2}\ \text{erg}, \quad (2)$$

where ϵ_γ is the radiation efficiency of the prompt emission, and $1-\epsilon_\gamma$ is of order of unity. The forward shock produced in the external medium enters a self-similar expansion phase with total shock energy $\simeq E_{\rm iso}$ soon after $t = t_d$ (Blandford & McKee 1976), as illustrated in Fig. 1. If we were to observe a burst at redshift $z \gtrsim 10$ with $E_{\rm iso} \gtrsim 10^{57}$ erg, and with a self-similar phase starting at $t_{d,\rm obs} = t_d(1+z) \gtrsim$ 1 day, this would very likely be a burst from a Pop. III VMS with $M_* \gtrsim 300\ M_\odot$.

3. Prompt photospheric emission

Pop. III GRB jets are likely to be dominated by Poynting-flux, as discussed in Section 2. The jet may have a subdominant thermal energy component of electron-positron pairs and photons, so that the emission from the photosphere can be bright. In addition to this, above the photosphere, the magnetic field could be directly converted into radiation via magnetic reconnection or the field energy could be converted into particle kinetic energy which can produce non-thermal radiation via shocks. The existence of the latter emission components is uncertain and they are currently difficult to model. Thus, for simplicity we focus on the photospheric emission, which is essentially unavoidable. Such photospheric emission models of the prompt emission are viable also for baryonic jets, which could work for Pop. I/II GRBs (e.g., Toma et al. 2011b). MR10 developed the Poynting-dominated jet model for a Pop. III GRB jet, and estimated the luminosity and temperature of the photospheric emission (see also Toma et al. 2011a).

Then we have the photon fluences in 64 s in the $15-50$ keV band for the isotropic luminosity $L_{\rm iso} = 4.4 \times 10^{53}$ erg s^{-1} and the base radius $r_l = 2R_h \simeq 9.4 \times 10^7 M_{h,2.5}$ cm of the jet as $S_{\rm ph} \simeq 1.4$ ph cm^{-2} for the case of $1+z = 20$ and $\simeq 1.3$ ph cm^{-2} for the case of $1+z = 10$.

A reasonable detection threshold of *Swift* BAT can be estimated by focusing on the image trigger mode, since it is based on a criterion with a fixed time-scale and energy band, while more general BAT threshold including the usual rate trigger is too complicated to estimate. The image trigger mode may be suitable for detecting weak and less-variable bursts like very-high-redshift bursts. We have used the samples in the BAT2 catalog (Sakamoto et al. 2011) and deduced the detection threshold of the BAT image trigger to be ~ 1 ph cm^{-2} for the 64 s interval in the $15-50$ keV band (Toma et al. 2011a). Thus the photospheric emission of Pop. III GRBs can marginally trigger BAT.

4. Very Early Afterglow

Rough predictions for the observational properties of the afterglows of Pop. III GRBs were made in MR10. The external shock driven by the jet in the circumburst medium powers the afterglow, which can be studied independently of the prompt emission (e.g., Sari et al. 1998). This is true whether the jet is baryonic or

Poynting-dominated, the jet acting simply as a piston. The external shock model of the GRB afterglows seems to be robust, since it (or a simple extension of the model) can explain many of the multi-band afterglows detected so far (e.g., Liang et al. 2007; De Pasquale et al. 2010).

We focus on the external shock emission at the observer's time $t_{\rm obs} \simeq t_{d,\rm obs}$, near the beginning of the self-similar expansion phase of the shock, when the emission is bright and may not be hidden by the prompt emission (see Fig. 1). The model is described in Toma et al. (2011a). Calculations of the external shock emission spectrum involve the parameters $E_{\rm iso}$ and t_d, as well as the external medium number density n, the fractions ϵ_B and ϵ_e of the thermal energy in the shocked region that are carried by the magnetic field and the electrons, respectively, and the index p of the energy spectrum of the accelerated electrons. The circumburst medium density in the very high-redshift universe is likely to be $n \gtrsim 0.1\ \rm cm^{-3}$. The microphysical parameters may be independent of $E_{\rm iso}, t_d$, or n as long as the shock velocity is highly relativistic, so that ϵ_B, ϵ_e, and p are thought to be similar to those for the bursts observed so far. Those have been constrained by fitting the late-time afterglows through models. The parameters related to the electrons are constrained relatively tightly as $\epsilon_e \sim 0.1$ and $p \sim 2.3$, while those for the magnetic field are not so tightly constrained, although typically for many afterglows $10^{-3} \lesssim \epsilon_B \lesssim 10^{-1}$ (e.g., Panaitescu & Kumar 2002).

The external shock emission at $t_{d,\rm obs}$ will have two intrinsically different cases, depending on the significance of the electron-positron pair creation within the emitting region. These cases are characterized by a negligible pair production regime and a significant pair production regime, which we show examples of spectra separately below.

An example of the negligible pair production case is obtained for the parameters $(E_{57.6}, t_{d,4}, n_0, \epsilon_{B,-2}, \epsilon_{e,-1}, f(p)) = (1, 1, 1, 1, 1, 1)$, where the notation $Q = 10^x Q_x$ in cgs units has been adopted ($E_{57.6} = E_{\rm iso}/10^{57.6}$ erg). The overall observer-frame spectrum for this case is shown in

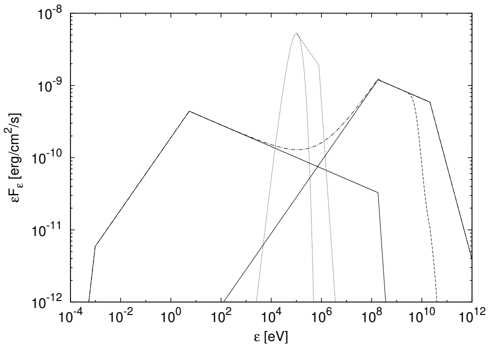

Fig. 2. Example of the observer-frame spectrum of a Pop. III GRB at the time $t_{d,\rm obs}$ when the jet activity ends, for the case of negligible intra-source pair production. The parameters are $E_{57.6} = t_{d,4} = n_0 = \epsilon_{B,-2} = \epsilon_{e,-1} = f(p) = 1$, and the source redshift $1 + z = 20$. The $\gamma\gamma$ absorption due to the EBL is expected to become significant at $\varepsilon > \varepsilon_{\rm EBL} \simeq 7$ GeV (Inoue et al. 2010), as shown by the dashed line. The dotted line represents the prompt emission's dominant photospheric black-body component with a possible power-law extension (see Section 3).

Figure 2. Since $\varepsilon_{\gamma\gamma} > \varepsilon_m^{\rm SC}$, most of the SSC emission is observed without being converted into e^+e^- within the emitting region.

Even photons escaping without attenuation within the emitting region can be absorbed by interacting with the extragalactic background light (EBL) ($\gamma\gamma \to e^+e^-$). Inoue et al. (2010) use a semi-analytic model of the evolving EBL and expect that high-energy photon absorption by the EBL for an arbitrary source at $z \simeq 20$ is significant at $\varepsilon > \varepsilon_{\rm EBL} \simeq 7$ GeV. For the parameters adopted here, $\varepsilon_{\gamma\gamma}$ is larger than $\varepsilon_{\rm EBL}$, which precludes obtaining intrinsic information about the emitting region from the observation of the $\gamma\gamma$ break.

An example of the case of significant pair production is obtained with the parameter set $(E_{57.6}, t_{d,4}, n_0, \epsilon_{B,-2}, \epsilon_{e,-1}, f(p)) = (1, 1, 10^2, 1, 2, 1)$. The overall observer-frame spectrum for this case is shown in Fig. 3 of Toma et al. (2011a). Most of the SSC emission is absorbed within the emitting region. The created pairs also emit synchrotron and inverse Compton emission. The important point of this case is that one will be able to detect a spectral break at energy $\varepsilon_{\gamma\gamma}$ due to pair creation *within* *the emission region* in the *Fermi* LAT energy range, 50 MeV - 30 GeV. This is a unique feature of GRB afterglows with very large $E_{\rm iso}$ (as expected for Pop. III GRB) and modest to large external density n. This is in contrast to the usual case of Pop. I/II GRBs, where the $\gamma\gamma$ self-absorption energy is not relevant for observations. The detection of $\varepsilon_{\gamma\gamma}$ will allow us to constrain the parameter n (for more details, see Toma et al. 2011a).

We can estimate the detection thresholds in the high energy ranges from the joint observation of GRB 090510 by *Swift* and *Fermi* (De Pasquale et al. 2010). This indicates that the thresholds of the 1-day averaged $\varepsilon F_\varepsilon$ flux are $\sim 6\times10^{-15}$ erg cm^{-2} s^{-1} in the XRT energy range 0.3 - 10 keV, $\sim 3\times10^{-10}$ erg cm^{-2} s^{-1} in the BAT energy range 15 - 150 keV, and $\sim 3\times10^{-11}$ erg cm^{-2} s^{-1} in the LAT energy range 50 MeV - 30 GeV. Compared to the results shown above, it appears that the thresholds of the XRT and LAT are thus sufficiently low to observe the high-energy spectrum of the external shock emission of Pop. III GRB.

The jet duration timescale t_d can be estimated from the steepening of the afterglow light curve and/or end of the prompt emission. A lower bound on the total isotropic energy $E_{\rm iso}$ can be estimated from the observed flux level in a specific energy range (Toma et al. 2011a).

5. Late-Time Radio Afterglows

We have focused so far on the high-energy emission just before and near the beginning of the external shock self-similar phase ($t_{\rm obs} \simeq t_{d,\rm obs}$) to examine their detectability by several instruments. In this section, we argue that the radio afterglows of Pop. III GRBs in the self-similar phase ($t_{\rm obs} > t_{d,\rm obs}$) can be so bright that they also provide powerful tools for constraining the event rate. At $t_{d,\rm obs}$, the flux of the external shock emission shown in Figure 2 at $\nu_a \simeq 230\ E_{57.6}^{1/6} t_{d,4}^{-1/2} n_0^{1/6} [(1+Y)/3.7]^{-1/3} [(1+z)/20]^{-1}$ GHz is given by $F_{\nu_a} \simeq 2.6\ \epsilon_{B,-2}^{-1/4} E_{57.6}^{2/3} n_0^{-1/12} [(1+Y)/3.7]^{-5/6} [(1+z)/20] d_{L,20}^{-2}$ Jy. *This indicates that the Pop. III GRB afterglows can be very bright radio sources, despite their large distances.*

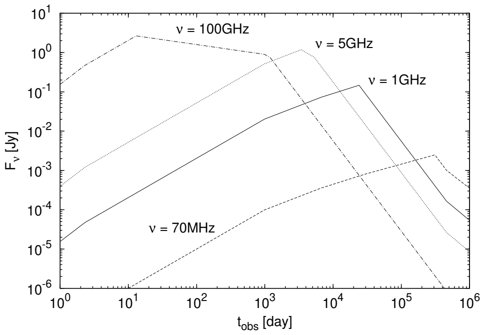

Fig. 3. Radio light curves at frequencies, 100 GHz (dot-dashed line), 5 GHz (dotted line), 1 GHz (solid line), and 70 MHz (dashed line), of a Pop. III GRB at $1+z=20$ with typical parameters $E_{57.6} = t_{d,4} = n_0 = \epsilon_{B,-2} = \epsilon_{e,-1} = f(p) = \theta_{j,-1} = 1$. The important observer's times are the jet duration $t_{d,\rm obs} \simeq 2.3$ day, the jet break time $t_{\theta,\rm obs} \simeq 9.9\times10^2$ day, and the time when the shock becomes non-relativistic $t_{\rm NR,obs} \simeq 4.6\times10^5$ day.

We briefly compute the light curves at various frequencies in the radio bands, 100 GHz, 5 GHz, 1 GHz, and 70 MHz, in our fiducial case, $E_{57.6} = t_{d,4} = n_0 = \epsilon_{B,-2} = \epsilon_{e,-1} = f(p) = \theta_{j,-1} = 1$. For calculating the radio emission we need to compute only the synchrotron emission of the original electrons. At late times, the number of pairs is typically small, and the pair emission is negligible. The SSC emission is not relevant in the radio bands. The results are plotted in Figure 3.

Figure 3 shows that the radio afterglows of Pop. III GRBs can be very bright with a very long duration. These could have been detected as quasi-steady point sources by the radio survey observations. As far as we know, the current largest radio survey data is based on the Very Large Array (VLA) FIRST survey (White et al. 1997), which observed a large area mainly around the north Galactic cap at 1.4 GHz, covering $\sim 1/5$ of all the sky. For the threshold, ~ 6 mJy at 1.4 GHz, a Pop. III GRB radio afterglow at $1+z=20$ (at $1+z=10$) can be observed for $t_{rd,\rm obs} \sim 300$ yr (for $t_{rd,\rm obs} \sim 200$ yr). Therefore, if we denote by $R_{w,4\pi}$ the all-sky Pop. III GRB rate in unit of

yr^{-1}, the number of the Pop. III radio afterglows that would have been detected in that survey is estimated to be $\sim (R_{w,4\pi}/5)t_{rd,\mathrm{obs}} \sim 10\ (R_{w,4\pi}/0.2\ \mathrm{yr}^{-1})(t_{rd,\mathrm{obs}}/300\ \mathrm{yr})$ for bursts at $1 + z \sim 20$. A detailed analysis of the FIRST data would thus provide a powerful constraint on $R_{w,4\pi}$ of Pop. III GRBs such as discussed in this paper (even no sources like our model calculations would provide an upper limit on the rate).

Levinson et al. (2002) and Gal-Yam et al. (2006) did not find any radio transient sources like GRB afterglows with timescales of significant flux changes of ~ 5 yr by comparing between the NVSS (spanned over 1993-1996) and FIRST (1994-2001) catalogs, which effectively cover $\sim 1/17$ of the sky. This indicates that $R_{w,4\pi} \lesssim 17/5 \sim 3\ \mathrm{yr}^{-1}$.

We also find that Pop. III GRB radio afterglows are so bright that they could be interesting background source candidates for 21 cm absorption line detections (Toma et al. 2011a).

6. Discussion

Putting constraints on the properties of Pop. III stars has recently become of great importance in modern cosmology. Planned IR surveys will be able to probe Pop. III stars. However, it is difficult to distinguish between a single Pop. III VMS and a cluster of less massive Pop. III stars. Thus, the detection of GRBs with very high E_{iso} and very long t_d could provide critical, 'smoking gun' evidence for the existence of VMSs. Multi-wavelength observations of such GRBs with *Swift*, *Fermi*, and ground-based IR and radio telescopes should provide us with invaluable information on Pop. III stars and their environments. We have also found that neutrinos from the Pop. III VMSs might be detectable (Gao et al. 2011).

One of the major potential problems is the formation rate of the Pop. III VMSs. Very recent calculations of the star formation rates imply that Pop. III VMSs might be very rare objects (e.g., De Souza et al. 2011).

Acknowledgements. I would like to thank the organizers for the good conference and giving me a chance to talk about our work. We acknowledge NASA NNX09AT72G, NASA NNX08AL40G, and NSF PHY-0757155 for partial support.

References

Blandford, R. D., & McKee, C. F. 1976, Phys. Fluids, 19, 1130
Blandford, R. D., & Znajek, R. L. 1977, MNRAS, 179, 433
Ciardi, B., & Ferrara, A. 2005, Space Sci. Rev., 116, 625
Cucchiara, A., et al. 2011, ApJ, 736, 7
De Pasquale, M., et al. 2010, ApJ, 709, L146
De Souza, R. S., Yoshida, N., & Ioka, K. 2011, A&A, 533, 32
Fryer, C. L., Woosley, S. E., & Heger, A. 2001, ApJ, 550, 372 (FWR01)
Gal-Yam, A., et al. 2006, ApJ, 639, 331
Gao, S., Toma, K., & Mészáros, P. 2011, PRD, 83, 103004
Greiner, J., et al. 2009, ApJ, 693, 1610
Inoue, S., et al. 2010, MNRAS, 404, 1938
Kawai, N., et al. 2006, Nature, 440, 184
Komissarov, S. S., & Barkov, M. V. 2010, MNRAS, 402, L25 (KB10)
Levinson, A., et al. 2002, ApJ, 576, 923
Liang, E. W., Zhang, B. B., & Zhang, B. 2007, ApJ, 670, 565
Mészáros, P., & Rees, M. J. 2010, ApJ, 715, 967 (MR10)
Nagakura, H., Suwa, Y., & Ioka, K. 2011, arXiv:1104.5691
Narayan, R., & Yi, I. 1994, ApJ, 428, L13
Panaitescu, A., & Kumar, P. 2002, ApJ, 571, 779
Sakamoto, T., et al. 2011, ApJS, 195, 2
Salvaterra, R., et al. 2009, Nature, 461, 1258
Sari, R., Piran, T., & Narayan, R. 1998, ApJ, 497, L17
Suwa, Y., & Ioka, K. 2010, ApJ, 726, 107
Tanvir, N. R., et al. 2009, Nature, 461, 1254
Toma, K., Sakamoto, T., & Mészáros P. 2011a, ApJ, 731, 127
Toma, K., Wu, X.-F., & Mészáros, P. 2011b, MNRAS, 415, 1663
White, R. L., et al. 1997, ApJ, 475, 479
Woosley, S. E. 1993, ApJ, 405, 273
Zalamea, I., & Beloborodov, A. M. 2011, MNRAS, 410, 2302